Nano hydroxyapatite structures influence early bone formation

Luiz Meirelles,[1,2] Anna Arvidsson,[2] Martin Andersson,[3] Per Kjellin,[3] Tomas Albrektsson,[2] Ann Wennerberg[1,2]

[1]*Department of Prosthetic Dentistry/Dental Material Science, Sahlgrenska Academy at Göteborg University, Göteborg, Sweden*

[2]*Department of Biomaterials, Sahlgrenska Academy at Göteborg University, Goteborg, Sweden*

[3]*Department of Applied Surface Chemistry, Chalmers University of Technology, Göteborg, Sweden*

Received 16 October 2006; revised 6 July 2007; accepted 31 July 2007
Published online 7 January 2008 in Wiley InterScience (www.interscience.wiley.com). DOI: 10.1002/jbm.a.31744

Abstract: In a study model that aims to evaluate the effect of nanotopography on bone formation, micrometer structures known to alter bone formation, should be removed. Electropolished titanium implants were prepared to obtain a surface topography in the absence of micro structures, thereafter the implants were divided in two groups. The test group was modified with nanosize hydroxyapatite particles; the other group was left uncoated and served as control for the experiment. Topographical evaluation demonstrated increased nanoroughness parameters for the nano-HA implant and higher surface porosity compared to the control implant. The detected features had increased size and diameter equivalent to the nano-HA crystals present in the solution and the relative frequency of the feature size and diameter was very similar. Furthermore, feature density per μm^2 showed a decrease of 13.5% on the nano-HA implant. Chemical characterization revealed calcium and phosphorous ions on the modified implants, whereas the control implants consisted of pure titanium oxide. Histological evaluation demonstrated significantly increased bone formation to the coated ($p < 0.05$) compared to uncoated implants after 4 weeks of healing. These findings indicate for the first time that early bone formation is dependent on the nanosize hydroxyapatite features, but we are unaware if we see an isolated effect of the chemistry or of the nanotopography or a combination of both. © 2008 Wiley Periodicals, Inc. J Biomed Mater Res 87A: 299–307, 2008

Key words: nanotopography; hydroxyapatite; osseointegration; *in vivo* test; bone healing; nano structures

INTRODUCTION

Integrity of the tissue/material interface is a fundamental requirement for success of oral and cement-free orthopaedic implants. Tissue material interaction is dependent on surface properties of used biomaterials together with host tissue responses. Surface properties involved in the early phase of wound healing are surface topography and chemical composition known to affect cell behavior[1–3] and subsequent tissue attachment to the implanted material.[4,5]

Correspondence to: L. Meirelles; e-mail: luiz.meirelles@odontologi.gu.se

Contract grant sponsors: CAPES, Swedish Research Council, Hjalmar Svensson Research Foundation, Wilhelm and Martina Lundgren Research Foundation and The Sylvan Foundation

The ultimate tissue response to the implanted material may depend on the adsorbed proteins that control cell migration and adhesion. Surface properties modulate the characteristics of the protein layer adhered[6,7] and such proteins are in the nanometer scale.[8] An *in vitro* research paper has demonstrated that 30 nm deep grooves were capable of inducing changes in cell spread and orientation.[9] Furthermore, nanoscale structures found in cell membranes have been characterized[10,11] and cell/tissue interactions are clearly influenced by structures at the nanometer level.[12,13]

Chemical modifications have also been implemented to modulate tissue reactions to the implanted material. Calcium phosphate (CaP) based materials have been intensively investigated due to their chemical similarity to bone minerals and potential bioactivity. Some CaP preparation techniques also produce hydroxyapatite, with a similar 3D structure to the bone. However, when used as a coating of metals, micron thick CaP materials may not resist stress levels resulting in de-attachment of

coating particles from the implant.[14] The alternative of thinner coatings, based on nanoparticles, may represent a way to avoid sequella from coat loosening.

To date, most *in vitro* studies have evaluated cell activity in relation to specific nanometer designs in forms of pits or grooves.[15,16] Observed cell alignment to the nanostructures is in accordance to the contact guidance phenomenon. However, the implementation of nanostructures on the surface may alter the surface roughness as well and some reports demonstrated that surface nanoroughness influence protein adhesion,[17] cell adhesion[18–20] and proliferation.[21] However, *in vitro* models to test cell interactions to nanostructured materials represent an artificial environment in lack of 3D cellular and extracellular reactions, blood flow, loading, and humoral influences to mention a few differences to the *in vivo* situation. Therefore, the precise relevance of *in vitro* findings may sometimes be difficult to conclude.

The present objective was to determine, *in vivo*, early bone response (4 weeks) to electropolished titanium implants modified with nanocrystalline hydroxyapatite. Histomorphometrical analyses were performed of bone in contact (BIC) and bone area adjacent to the implant in a rabbit model. Implant surface analyses were used to verify chemical compositions and to evaluate the topography at the micro and nanoscale, determining the dimensions of the topographical features present at the surface and calculating the surface roughness parameters. To the knowledge of the authors, this is the first experiment to evaluate *in vivo* bone response to nanostructured modified implants.

MATERIAL AND METHODS

Implants and stabilization plate

Cylindrical implants measuring 8 mm in length and 3.5 mm in diameter were made from commercially pure (cp) titanium rods (grade 3). Each implant had a threaded part on the top screwed through a plate to achieve full fixation. The plate consisted of two side holes for the fixating screws and a threaded central hole for the tested implants (Fig. 1). This model provides the same fixation to the implant no matter the surface properties and prevents uncontrolled micromovements that may cause soft tissue integration of the very smooth implant used in this study. The osteosynthesis plate was developed to ensure maximal stability enabling *in vivo* observations of the microcirculation of grafted bone[22] and has been used in several studies.[23–25] The superior cylindrical part of the implant was to be placed underneath the plate at the cortical level of tibia whereas the remaining inferior part of the implant was in the bone marrow. A total of 20 cylindrical implants were divided in two groups. One group (10 implants) served as control and had the surface electropolished (E) implants. The second group (10 implants) had electropolished surface and was further modified with nanocrystalline hydroxyapatite (E-HA) implants.

Implant surface modification

Electropolishing technique

The turned implants (as received) were topographically analyzed and microstructures were detected [Figs. 2(a) and 3(a)]. In order to remove the microstructures the implants were electropolished according to the procedure described by Piotrowski et al.[26] Briefly, the implants were immersed into an electrolyte consisting of a 3 M sulfuric acid in methanol, kept at -10°C. The implants were rotated at a rate of 300 rpm and a platinum wire, placed at a distance of 5 cm away from the implant, was used as a counter electrode. A potential of 7.75 V was applied for approximately 15 min.

HA nanocrystalline synthesis and titanium implants modification

Ten samples were surface modified with hydroxyapatite (HA) using the Promimic HA^{nano}-method, a detailed description can be found elsewhere.[27] The method results in nanocrystalline HA as observed in Figure 4. The implants were dipped into a stable particle suspension containing 10 nm in diameter HA particles followed by a heat treatment at 550°C for 5 min in nitrogen atmosphere. The surfactant mediated process allows better control of the chemical composition of the coating. The intimate mixture of the coating components allows lower processing temperatures preventing undesired phase transitions and a high homogeneity of the film is expected.[5] Surfactant mediated process can be used in more complex samples, requires considerably less equipment and is potentially less expensive than many the alternative coating techniques.

Topographical surface characterization

Topographical analyses were performed using optical interferometry (MicroXAM^{TM}, PhaseShift, Tucson, USA) and atomic force microscopy (AFM) (Dimension 3000 SPM^{TM}, Digital Instruments, Santa Barbara, USA), respectively. The optical interferometry has a lateral resolution of 0.3 μm and vertical resolution of 0.05 nm and is suitable to evaluate numerically microstructures. Higher resolution evaluation of nanostructures was performed with AFM, with lateral resolution of 2 nm and vertical resolution in the atomic level. For the optical interferometry analysis a measurement area of 200 × 260 μm (50× objective, zoom factor 0.625) was used and a Gaussian filter (size 50 × 50 μm) selected to remove errors of form. Three specimens of each type of implant were analysed at the top, middle and bottom part, making a total of 27 measurements for each group.

AFM analysis was performed in TappingMode^{TM} using etched silicon probes (Digital Instruments) with cantilever lengths of 125 nm and resonance frequencies of 270–310 kHz. A measurement area of 10 × 10 μm was used and

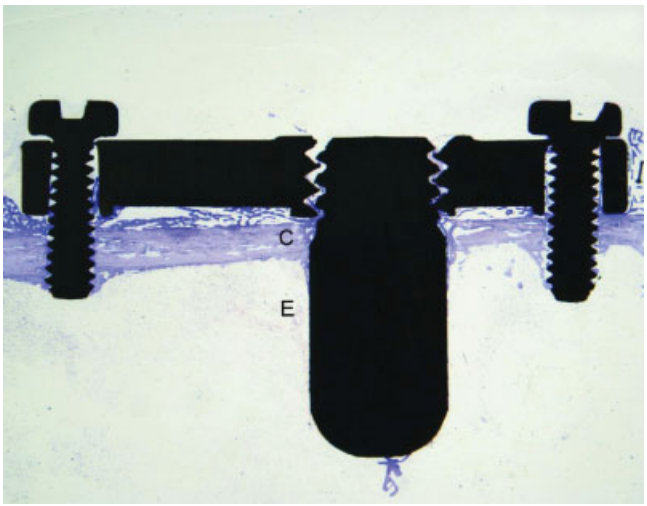

Figure 1. Titanium fixation plate with two side screws positioned in the rabbit tibia. External and internal thread design was used to ensure implant stability and adequate levelling to the cortical bone. Bone area measurements made on the cortical (C) and endosteal (E) region are marked. Ground section, ×1 magnification. [Color figure can be viewed in the online issue, which is available at www.interscience.wiley.com.]

the measurements were performed at a scan rate of 1.0 Hz on six different places. Errors of tilt and bow were removed with a third order least mean square fit (SPIP™, Image Analysis A/S, Denmark). The 3D roughness parameters calculated from both resolutions investigated were the arithmetic average height deviation (S_a), the density of summits (S_{ds}), and the developed surface ratio (S_{dr}). Mathematical descriptions of the parameters can be found in the literature.[28]

The AFM measurements were further analysed with a software processor package (Scanning Probe Image Processor, SPIP™, Image Analysis A/S) to characterize the surface structures configuration. This software performs automatic structure identification and provides the dimension for each distinct structure.[29] Grain analysis mode was used to identify the surface features diameter, size and number per μm^2. Pore analysis mode was used to identify the surface pores diameter, depth, and surface porosity (%).

Chemical surface characterization

The chemical composition of the implants surface was monitored using X-ray Photoelectron Spectroscopy (XPS) using a PHI 5500 (Perkin Elmer, Physical Electronics

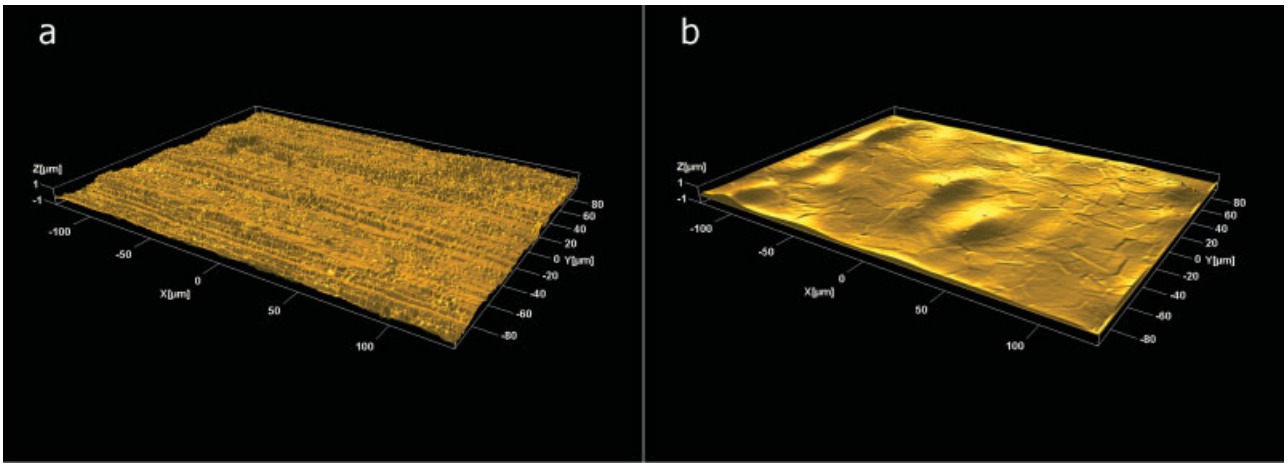

Figure 2. Interferometer images of the as received implant with micro structures (a) and the very smooth electropolished nano-HA implant revealing the grain boundaries (b). Measurement area of 200 × 260 μm. [Color figure can be viewed in the online issue, which is available at www.interscience.wiley.com.]

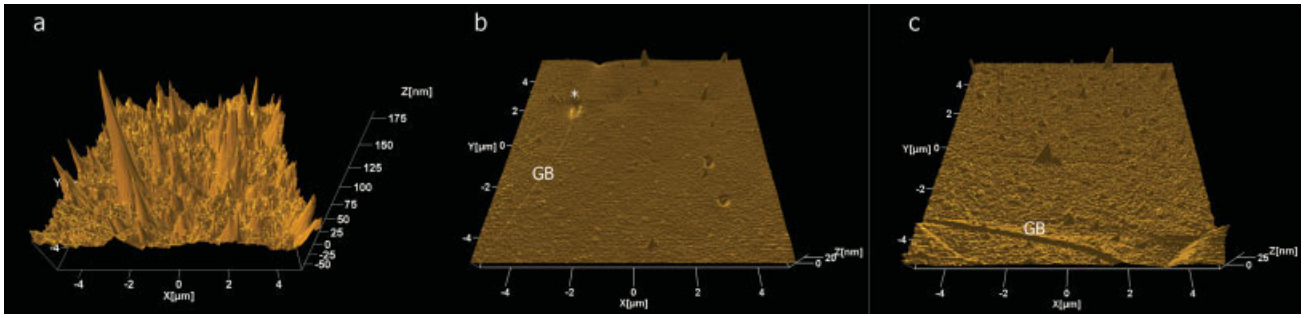

Figure 3. AFM 10 × 10 μm images of as received (a), electropolished (b) and electropolished + nano-HA (c) implant. Grain boundaries (GB) can be observed on (b) and (c). [Color figure can be viewed in the online issue, which is available at www.interscience.wiley.com.]

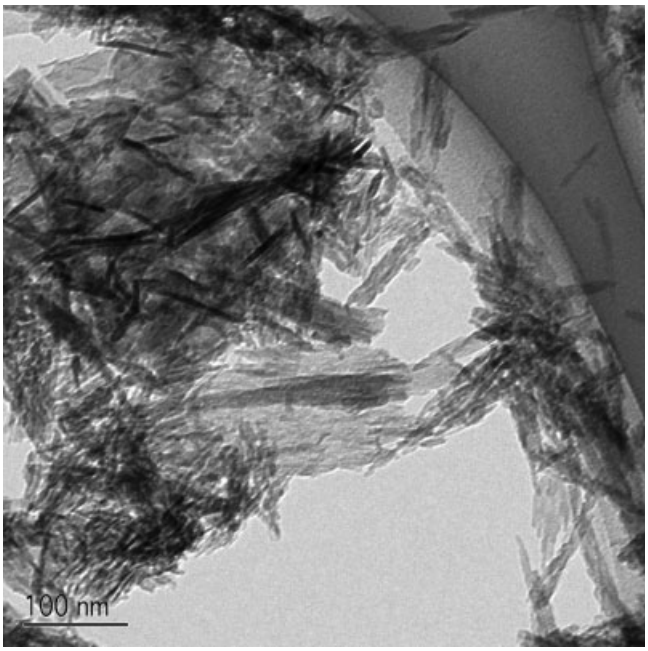

Figure 4. Morphology of the HA crystals by TEM.

Division). Monochromatic AlKα X-ray radiation operated at 350 W was utilized and the relative energy scale was fixed with C 1s.

Surgical technique

Ten female New Zealand rabbits, minimally 10 months old, were used in this study. They were kept in one specially designed room and allowed to run freely. The rabbits had free access to tap water and were fed with standard pellets. The study was approved by the local animal ethical committee at Göteborg University.

Animals were anaesthetized with intramuscular injections of fentanyl and fluanison (Hypnorm Vet, Janssen Farmaucetica, Belgium) at a dose of 0.5 mL per kg of body weight and intraperitoneal injections of diazepam (Stesolid, Dumex, Denmark) at a dose of 0.25 mg per animal. If necessary anaesthesia was maintained using additional doses of Hypnorm at a dose of 0.1 mL per kg body weight. Before surgery, the shaved skin of the rabbit was carefully washed with a mixture of 1% iodine and 70% ethanol. Local anesthesia with 1.0 mL of 5% lidocaine (Xylocain, Astra Zeneca, Sweden) was injected subcutaneously in the surgical site. A single dose of prophylactic antibiotic (Borgal, Intervet, Boxmeer, The Netherlands) was administered a dose of 0.5 mL per kg body weight. All 10 animals received 0.5 mL of an analgesic (Temgesic, Reckitt and Coleman, England) at a concentration of 0.3 mg/mL on the day of operation and 3 days there after.

Operations were performed under aseptic conditions. Three holes were drilled with a round burr on the flat proximal, medial tibial methaphysis surface parallel to the long axis of the bone. A sequence of twist drills was utilized to prepare the central hole with a final diameter of 3.5 mm that corresponds to the implant diameter, and the remaining two holes were to be placed as the side screws. This procedure was performed under copious saline irrigation at low rotatory speed. The implant connected to the fixating plate was positioned in the central hole and fastened against the cortical bone by two side screws (Fig. 1).

Histological analyses

Four weeks after surgery the animals were anaesthetized with intramuscular injections of fentanyl and fluanison (Hypnorm Vet, Janssen Farmaucetica, Belgium) at a dose of 0.5 mL per kg of body weight and further sacrificed with 10 mL overdose of pentobarbital 60 mg/mL, (Pentobarbitalnatrium, Apoteksbolaget, Sweden). The implants with surrounding tissues were removed en bloc and immersed in 4% neutral buffered formaldehyde. Twenty samples ($n = 10$ for each implant group) were processed to be embedded in light curing resin (Technovit 7200 VLC, Kulzer Wehrhein, Germany). Preparations of undecalcified cut and ground sections from the implants were performed with a sawing and grinding equipment.[30] A central section was taken from each sample and ground to an approximately 40-μm-thick section and stained with toluidine blue. The amount of titanium present in each section did not allow further grinding to thinner sections. Histological evaluations were carried out using a light microscope (Eclipse ME600, Nikon, Japan) and histomorphometrical data analyzed by an image analysis software (Image Analysis 2000, Tekno Optik AB,Sweden). Bone in contact (BIC) percentage was calculated along the entire implant and calculated with 10× objective magnification. Bone area percentage was calculated inside a rectangle area drawn with the implant surface as base and with a height of 150 μm as done previously on cylindrical implants[25,31] and separately analyzed for the cortical and endosteal regions, respectively (Fig 1).

Statistical analysis

To test if there were surface topographical differences in different regions of the same implant, surface roughness parameters were calculated in the top, middle, and bottom parts and statistical analysis was then performed with the Kruskal-Wallis Test. Surface roughness parameters comparison between the E and E-HA implants were performed with the Mann-Whitney Test. For the histomorphometric evaluation between the two groups, the Wilcoxon sign rank test was used. Significance level considered was $p \leq 0.05$.

RESULTS

Topographical surface characterization

Optical interferometry images of both E and E-HA implants revealed very smooth surfaces and the presence of titanium grain boundaries [Fig. 2(b)]. Surface roughness parameters measured in the

TABLE I
Optical Interferometry Roughness Parameters Comparison Within Each Group on the Three Regions Evaluated[a] and Between Electropolished and Electropolished Nano-HA Implants[b]

	Electropolished					Electropolished-HA					
	Top	Middle	Bottom	p Value[a]	Mean	Top	Middle	Bottom	p Value[a]	Mean	p Value[b]
S_a (nm)	109.3	94.3	78.9	NS	94.2 ± 71.6	128.6	141.4	133.3	NS	134.4 ± 55.4	0.03
S_{ds} (μm^{-2})	0.01	0.02	0.02	NS	0.01 ± 0.0	0.01	0.02	0.02	NS	0.01 ± 0.0	NS
S_{dr} (%)	0.07	0.07	0.04	NS	0.06 ± 0.1	0.18	0.31	0.47	NS	0.32 ± 0.4	0.00

[a]Kruskal-Wallis Test ($p \leq 0.05$).
[b]Mann-Whitney Test ($p \leq 0.05$).

implant top, middle and bottom part were compared and revealed similar mean values, exhibiting a homogenous surface along the entire implants in both groups (Table I). A second evaluation compared surface roughness between the E and E-HA implants. S_{ds} parameter calculated showed similar values, whereas the S_a and S_{dr} parameters showed higher nanometer values for the E-HA group (Table I).

Surface roughness parameters calculated at higher resolution with AFM exhibited also increased S_a and S_{dr} parameters at the nanometer level for the E-HA implants compared to the E implants (Table II), whereas the S_{ds} were slight higher for the E implants. Following surface roughness calculation, the topographical features detected with the AFM were characterized (Fig. 3). Surface pore analysis of the implants showed increased mean value of 669 pores and higher coverage area of 7.2% for the E-HA implant compared to the E implant, with 29 pores and coverage area of 2.3%. The few pores present at the E implant surfaces had greater diameter of 151 nm and increase depth of 2.6 nm compared to 82.9 and 1.3 nm of the E-HA implants, respectively (Table II).

The range of differences found in the pore dimensions was not observed in the grain analysis. E implant exhibited an increase of 104 features per μm^2 compared to 90 features per μm^2 for the E-HA implant. Feature size and diameter mean values calculated for the E implant was 86.2 ± 86.6 and 61.3 ± 40, while the mean values for the E-HA implant was 93.3 ± 99.9 and 66.9 ± 54.3, respectively. In addition, there was a very similar frequency (measured as percentage) of the different diameters of the detected features (Fig. 5).

Chemical surface characterization

XPS spectra of the two surface types (E and E-HA) are presented in Figure 6. The electropolished surface consisted of pure titanium oxide [Fig. 6(a)] compared to the HA modified sample, which had peaks originating from calcium and phosphorus present [Fig. 6(b)]. No pronounced differences in the carbon contents could be observed, i.e. the HA modification step did not leave any additional carbon on the surface. Furthermore the calcium to phosphorous ratio was measured to be approximately 1.2, which corresponds to hydroxyapatite with some calcium deficiency, as reported recently on nano-HA based materials.[20,32] However, it should be noted that the accuracy of this technique is somewhat limited in terms of determining absolute amounts.

Animal follow-up

One animal died during surgery from unknown reasons. During the first week two animals bit the wound area and new sutures were applied. In these animals no signs of infection could be observed and they kept running throughout the healing period and were not excluded from the experiment.

Histological analysis

After 4 weeks, the histological specimens showed older cortical bone and darker stained newly formed bone. Newly formed bone stage development corresponded to the early healing period, with clear bone

TABLE II
AFM Roughness Parameters and Pore Analyses[a]

Implant	S_a (nm)	S_{ds} (μm^{-2})	S_{dr} (%)	n Pores	% Coverage	Diameter	Mean Z Value
E	0.9 ± 0.2	115 ± 25	0.0 ± 0.0	29 (8–39)	2.3 ± 1.4 (0.8–4.1)	151.6 ± 282.8 (31.2–1599)	2.6 ± 1.2 (1.7–32.6)
E-HA	2.3 ± 1.5	90 ± 23	0.4 ± 0.3	669 (248–1642)	7.2 ± 5.8 (2.4–18.6)	82.9 ± 78.7 (22.1–1057)	1.3 ± 0.4 (1.0–19.1)

[a]Given are mean values of the electropolished (E) and electropolished nano-HA (E-HA). Mean ± SD (range).

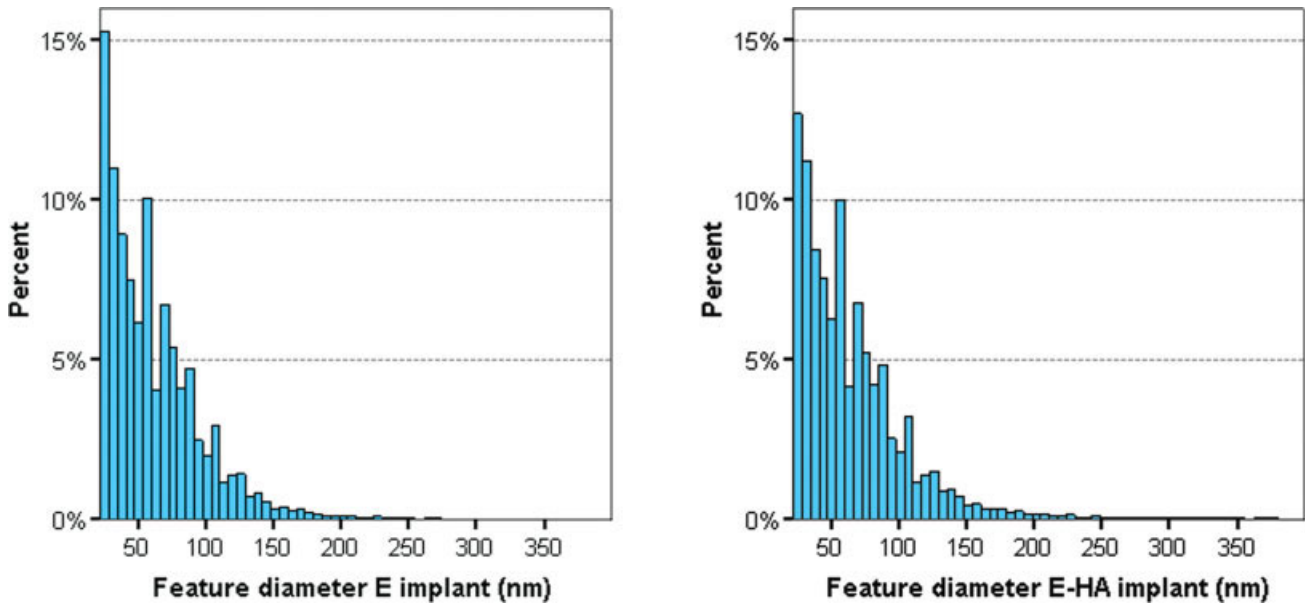

Figure 5. Feature diameter histograms detected on the AFM evaluation. The relevant difference observed is the decrease of 2.5% of the lower segment in diameter for the nano-HA implant due to the addition of HA crystals with dimensions in this range and the few more features detected in the range of 200–300 nm compared to the electropolished implant (left). Plotted values correspond to a cumulative percent of 99.8%. [Color figure can be viewed in the online issue, which is available at www.interscience.wiley.com.]

tissue distinguishing lines between the cortical lamellar bone and woven bone (Fig. 7).

Histomorphometric evaluations showed significantly higher bone in contact for the E-HA compared to E implants ($p = 0.038$). The mean percentage calculated was 9.0% ± 6.1% for the E-HA implants compared to 3.2% ± 3.6% for the E implants (Table III). Comparisons of the bone area in the cortical and endosteal region revealed similar values between E and E-HA implants. Values are presented in Table III.

DISCUSSION

This study demonstrated increased BIC values to electropolished nano-HA modified implants com-

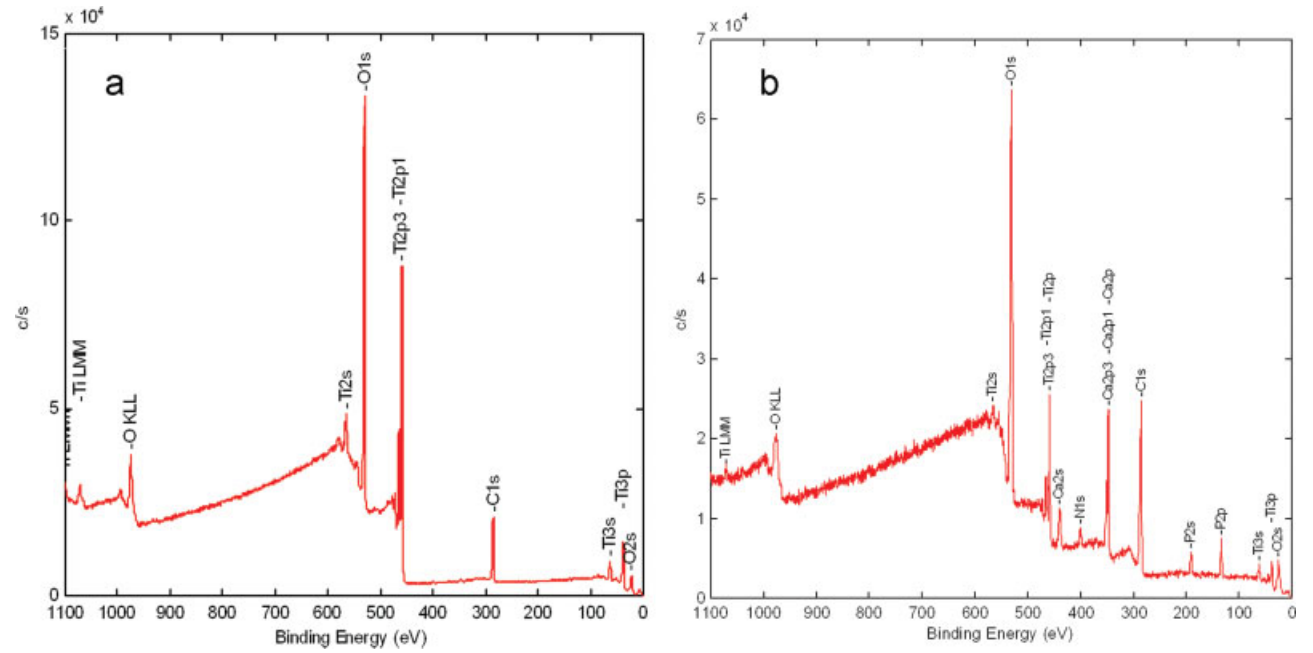

Figure 6. XPS analysis of as prepared electropolished samples without (a) and with (b) nano-HA. [Color figure can be viewed in the online issue, which is available at www.interscience.wiley.com.]

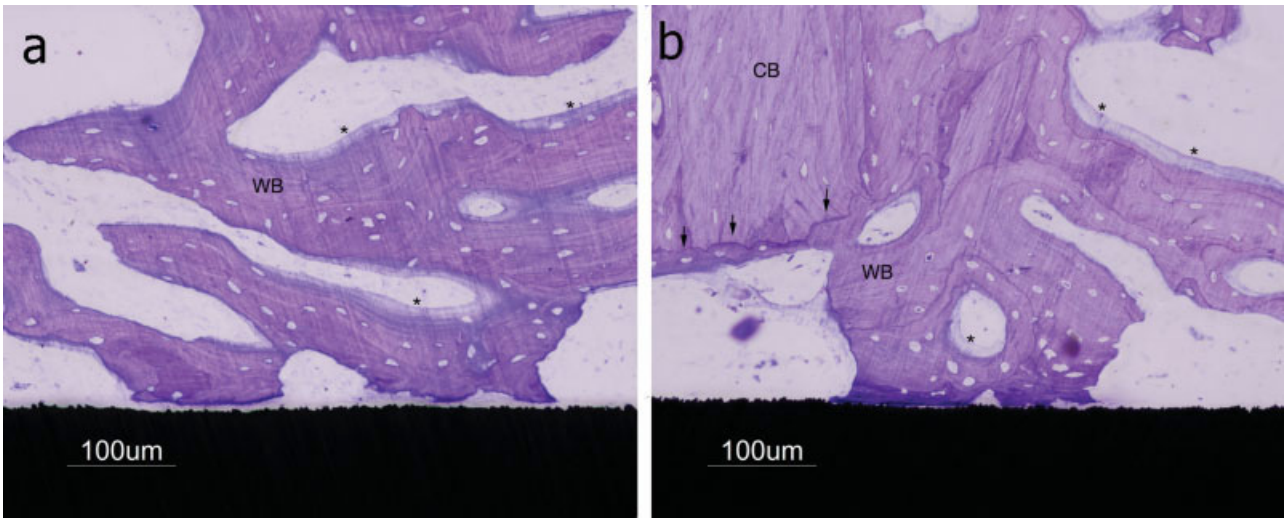

Figure 7. Ground section ×20 magnification of the implants. (a) E implant (uncoated) demonstrates less bone contact than (b) E-HA (coated) implant. Cortical lamellar bone (CB) edges with signs of resorption and new bone formed with a clear distinguishing line (arrows). Osteoblasts rim intense activity (*) is observed around the woven bone (WB). [Color figure can be viewed in the online issue, which is available at www.interscience.wiley.com.]

pared to electropolished implants. Chemical analyses revealed different surface composition for the two groups. While E-HA implants revealed calcium and phosphorous peaks on XPS spectra, E implants consisted of pure titanium oxide. Several reports have demonstrated that calcium phosphate (CaP) based materials affect early events at the tissue/material interface leading to increased bone formation on micron thick CaP layers.[33,34] The assumed ability to bond to bone tissue is a property of bioactive ceramics[35] and a possible explanation for our results. The characteristics of CaP materials that may improve bone tissue formation are, for example, dissolution of calcium and phosphate ions at the interface that could enrich the environment at the interface, forming carbonate apatite, an apatite similar to the one found in bone.[36] Some *in vitro* investigations of nano-HA showed increased osteoblast adhesion, probably mediated by specific protein adsorption followed by greater osteoblast proliferation.[17,21] In contrast, no differences were observed in osteogenic cell attachment and spreading on nano-HA coated and uncoated titanium samples.[18,20] Cells demonstrated well developed filopodia on the nano-HA implants, as observed previously on nanotextured titanium samples.[37] Such events occur prior to bone formation and a better understanding may explain the present higher bone in contact values for the nano-HA implants.

In this study, the BIC values found in both groups (Table III) were low compared to raw values of others studies investigating micrometer-rough surfaces. The present surfaces were extremely smooth at the micrometer scale (Table I), with the surface roughness parameters far from the optimal for bone formation.[38] While the BIC values calculated on the two implants were different, bone area measurements showed similar values.[39,40] One possibility is that the surface properties observed on the nano-HA implant alters the bone response at the interface and do not interfere with bone density at early stages, such as 4 weeks used in this study. Moreover, most reports from our group have found similar results, with different BIC but similar bone area values in other not related studies,[39–41] hence we are uncertain about the relevance of the bone area observations.

TABLE III
Bone Contact Percentage and Bone Area Percentage Measured on the Cortical and Endosteal Region of the Electropolished (E) and Electropolished Nano-HA (E-HA)[a]

Implant	BIC %	Cortical Region	Endosteal Region
E	3.2 ± 3.6 (1.1–12.6)	75.4 ± 15.1 (43.2–96.1)	39.1 ± 18.9 (12.4-72.1)
E-HA	9.0 ± 6.1 (2.8–20.0)	82.9 ± 11.0 (59.6–98.1)	38.1 ± 21.3 (11.4–79.0)
p value[b]	0.038	NS	NS

[a]Given are mean ± SD (range).
[b]Wilcoxon sign rank test ($p < 0.05$).

The surface features detected with AFM showed increased size and diameter mean values for the nano-HA implants when compared to the electropolished implants and such differences are compatible with the nano-HA particle used. However, this small difference could occur as result of few larger features present at the nano-HA implant due to the formation of crystal agglomerates, resulting in the same mean values found but with a different feature dimensions distribution. In order to verify this hypothesis the feature diameter distribution for both implants were calculated and the histogram of the relative frequency showed very similar percentage for each segment. The difference of 14 features per μm^2 calculated from E implants ($104/\mu m^2$) and E-HA implant ($90/\mu m^2$) may also influence early healing events. Some studies showed that cellular activity may depend on modifications of feature dimensions and density. A study used colloidal lithography to implement hemispherical nanopillars with a density of 11.8 μm^2, a diameter of 167 nm, and a height of 100 nm on Ti-coated silicon wafers,[15] a lower density and higher diameter compared to our study. T24 cells appeared less spread with more membrane protrusions and produced lower amounts of cytokines compared to flat samples[15]. In another study,[42] varying the hemispherical nanopillar density revealed that human osteoblast adhesion was maintained during the experiment on samples with 19% and 30% coverage area compared to the decrease of viable cells on the flat and 3% and 43% samples (extreme values). Thus, a decrease of 13.5% of the feature density on the nano-HA implant may contribute to enhance bone formation observed in the present study. However, nano-HA modification did not alter the frequency of feature dimensions on control and test implants and the increased mean values of the feature dimensions is equivalent to the nano-HA crystals present in the solution.

Surface porosity analysis revealed a different scenario. Higher porosity (%) and higher number of pores at the E-HA implant represent more binding sites for specific biomolecules that may adhere at the material surface in the early inflammatory stage. If so, this may further contribute to cell migration and proliferation very close to the implant surface, explaining the higher BIC values found on the E-HA compared to the E implant. Additionally, the difference observed in pore diameter and depth represents other alterations to explain the difference in bone formation, since E implants had wider and deeper pores compared to E-HA implants. Probably, the small HA particles can fill the wider pores of the underlying substrate and at the same time increase the number of the small pores. These findings are relevant since cell behavior and probably further tissue formation is affected by the structure dimensions and distribution at the nanometer scale,[12,13] known as the contact guidance phenomenon.

The surface roughness parameters calculated from the AFM measurements showed higher S_a and S_{dr} values on the E-HA implant compared to E implant and can be explained by the increased surface porosity that would lead to increased surface arithmetic high deviation (S_a) and developed surface area (S_{dr}). The similar density of summits values (S_{ds}) are related to the similar surface structure dimensions and relative frequency of both implants investigated at this resolution. By coating a rougher sample, such as anodised[20] or blasted,[43] surface roughness is likely to decrease with the nano-HA crystals, broadening the peaks and filling the pores and grooves. In the present study, the underlying surface was very smooth (electropolished) and the added HA nanocrystals increased the surface roughness of the implant. However, the level of optimal surface roughness for bone formation at the nanoscale remains poorly investigated and it is unknown if the differences found could affect the overall tissue formation. More experiments must be done to establish the ideal topographical dimensions and frequency at the surface and to understand the mechanisms behind the difference in bone response.

In conclusion, this experimental study provided the first evidence *in vivo* of enhanced bone response to nano-HA modified titanium implants. Implant surface modifications were applied to ensure that the microstructures were removed and observed tissue formation was determined by the presence of the nano-HA features. Differences in surface chemical composition and nanotopography were detected between the electropolished and nanostructured HA implants that explain the difference in bone formation. Future studies should address separately the potential bioactivity of HA coating effect and the importance of nanostructures present at the material surface to the overall tissue response.

References

1. Curtis A, Wilkinson C. Topographical control of cells. Biomaterials 1997;18:1573–1583.
2. Boyan BD, Hummert TW, Dean DD, Schwartz Z. Role of material surfaces in regulating bone and cartilage cell response. Biomaterials 1996;17:137–146.
3. Chehroudi B, Gould TR, Brunette DM. Effects of a grooved titanium-coated implant surface on epithelial cell behavior in vitro and in vivo. J Biomed Mater Res 1989;23:1067–1085.
4. Wennerberg A. Biomaterials Science/Handicap Research. Göteborg: Göteborg University; 1996.
5. Gottlander M, Johansson CB, Wennerberg A, Albrektsson T, Radin S, Ducheyne P. Bone tissue reactions to an electrophoretically applied calcium phosphate coating. Biomaterials 1997;18:551–557.

6. Walivaara B, Aronsson BO, Rodahl M, Lausmaa J, Tengvall P. Titanium with different oxides: In vitro studies of protein adsorption and contact activation. Biomaterials 1994;15:827–834.
7. Ellingsen JE. A study on the mechanism of protein adsorption to TiO_2. Biomaterials 1991;12:593–596.
8. Hay ED. Cell Biology of Extracellular Matrix. New York: Plenum; 1991.
9. Wojciak-Stothard B, Curtis A, Monaghan W, MacDonald K, Wilkinson C. Guidance and activation of murine macrophages by nanometric scale topography. Exp Cell Res 1996;223:426–435.
10. Shirato I, Tomino Y, Koide H, Sakai T. Fine structure of the glomerular basement membrane of the rat kidney visualized by high-resolution scanning electron microscopy. Cell Tissue Res 1991;266:1–10.
11. Abrams GA, Goodman SL, Nealey PF, Franco M, Murphy CJ. Nanoscale topography of the basement membrane underlying the corneal epithelium of the rhesus macaque. Cell Tissue Res 2000;299:39–46.
12. Curtis A, Wilkinson C. New depths in cell behaviour: Reactions of cells to nanotopography. Biochem Soc Symp 1999;65:15–26.
13. Flemming RG, Murphy CJ, Abrams GA, Goodman SL, Nealey PF. Effects of synthetic micro- and nano-structured surfaces on cell behavior. Biomaterials 1999;20:573–588.
14. Bloebaum RD, Beeks D, Dorr LD, Savory CG, DuPont JA, Hofmann AA. Complications with hydroxyapatite particulate separation in total hip arthroplasty. Clin Orthop Relat Res 1994:19–26.
15. Andersson AS, Backhed F, von Euler A, Richter-Dahlfors A, Sutherland D, Kasemo B. Nanoscale features influence epithelial cell morphology and cytokine production. Biomaterials 2003;24:3427–3436.
16. Teixeira AI, Abrams GA, Bertics PJ, Murphy CJ, Nealey PF. Epithelial contact guidance on well-defined micro- and nanostructured substrates. J Cell Sci 2003;116:1881–1892.
17. Webster TJ, Ergun C, Doremus RH, Siegel RW, Bizios R. Specific proteins mediate enhanced osteoblast adhesion on nanophase ceramics. J Biomed Mater Res 2000;51:475–483.
18. Zhu X, Eibl O, Scheideler L, Geis-Gerstorfer J. Characterization of nano hydroxyapatite/collagen surfaces and cellular behaviors. J Biomed Mater Res A 2006;79:114–127.
19. Webster TJ, Siegel RW, Bizios R. Osteoblast adhesion on nanophase ceramics. Biomaterials 1999;20:1221–1227.
20. Zhu XL, Eibl O, Berthold C, Scheideler L, Geis-Gerstrofer J. Structural characterization of nanocrystalline hydroxyapatite and adhesion of pre-osteoblast cells. Nanotechnology 2006;17: 2711–2721.
21. Webster TJ, Ergun C, Doremus RH, Siegel RW, Bizios R. Enhanced functions of osteoblasts on nanophase ceramics. Biomaterials 2000;21:1803–1810.
22. Albrektsson T, Albrektsson B. Microcirculation in grafted bone. A chamber technique for vital microscopy of rabbit bone transplants. Acta Orthop Scand 1978;49:1–7.
23. Albrektsson T. Repair of bone grafts. A vital microscopic and histological investigation in the rabbit. Scand J Plast Reconstr Surg 1980;14:1–12.
24. Carlsson L, Rostlund T, Albrektsson B, Albrektsson T. Implant fixation improved by close fit. Cylindrical implant-bone interface studied in rabbits. Acta Orthop Scand 1988; 59:272–275.
25. Meirelles L, Arvidsson A, Albrektsson T, Wennerberg A. Increased bone formation to nano rough unstable implant. Clin Oral Implants Res 2007;18:326–332.
26. Piotrowski O, Madore C, Landolt D. The mechanism of electropolishing of titanium in methanol-sulfuric acid electrolytes. J Electrochem Soc 1998;145:2362–2369.
27. Kjellin P, Andersson M. SE-0401524-4, assignee. Synthetic nano-sized crystalline calcium phosphate and method of production patent SE527610. 2006. 25 April 2006.
28. Stout K-J SP, Dong WP, Mainsah E, Luo N, Mathia T, Zahouani H. The development of methods for characterization of roughness in three dimensions. EUR 15178 EN of Commission of the European Communities, University of Birmingham, Birmingham; 1993.
29. Pellechia PJ, Gao JX, Gu YL, Ploehn HJ, Murphy CJ. Platinum ion uptake by dendrimers: An NMR and AFM study. Inorg Chem 2004;43:1421–1428.
30. Donath K. Preparation of histologic sections by cutting-grinding technique for hard tissue and other materials not suitable to be sectioned by routine methods. Norderstedt: Exakt-Kulzer; 1993. p 1–16.
31. Hallgren C, Sawase T, Ortengren U, Wennerberg A. Histomorphometric and mechanical evaluation of the bone-tissue response to implants prepared with different orientation of surface topography. Clin Implant Dent Relat Res 2001;3: 194–203.
32. Jager C, Welzel T, Meyer-Zaika W, Epple M. A solid-state NMR investigation of the structure of nanocrystalline hydroxyapatite. Magn Reson Chem 2006;44:573–580.
33. Cook SD, Thomas KA, Dalton JE, Volkman TK, Whitecloud TS III, Kay JF. Hydroxylapatite coating of porous implants improves bone ingrowth and interface attachment strength. J Biomed Mater Res 1992;26:989–1001.
34. Gottlander M, Albrektsson T. Histomorphometric studies of hydroxylapatite-coated and uncoated CP titanium threaded implants in bone. Int J Oral Maxillofac Impl 1991;6:399–404.
35. Jarcho M. Calcium phosphate ceramics as hard tissue prosthetics. Clin Orthop Relat Res 1981:259–278.
36. LeGeros RZ. Biodegradation and bioresorption of calcium phosphate ceramics. Clin Mater 1993;14:65–88.
37. de Oliveira PT, Nanci A. Nanotexturing of titanium-based surfaces upregulates expression of bone sialoprotein and osteopontin by cultured osteogenic cells. Biomaterials 2004; 25:403–413.
38. Albrektsson T, Wennerberg A. Oral implant surfaces, Part 1: Review focusing on topographic and chemical properties of different surfaces and in vivo responses to them. Int J Prosthodont 2004;17:536–543.
39. Wennerberg A, Albrektsson T, Lausmaa J. Torque and histomorphometric evaluation of c.p. titanium screws blasted with 25- and 75-microns-sized particles of Al2O3. J Biomed Mater Res 1996;30:251–260.
40. Sul YT, Johansson CB, Roser K, Albrektsson T. Qualitative and quantitative observations of bone tissue reactions to anodised implants. Biomaterials 2002;23:1809–1817.
41. Wennerberg A, Albrektsson T, Johansson C, Andersson B. Experimental study of turned and grit-blasted screw-shaped implants with special emphasis on effects of blasting material and surface topography. Biomaterials 1996;17: 15–22.
42. Rice JM, Hunt JA, Gallagher JA, Hanarp P, Sutherland DS, Gold J. Quantitative assessment of the response of primary derived human osteoblasts and macrophages to a range of nanotopography surfaces in a single culture model in vitro. Biomaterials 2003;24:4799–4818.
43. Meirelles L, Currie F, Jacobsson M, Albrektsson T, Wennerberg A. The effect of chemical and nanotopographical modifications on early stage of osseointegration. Int J Oral Maxillofac Surg. Submitted for publication. Int J Oral Maxillofac Implants. Forthcoming.